bending moments and dynamic lateral earth pressures on the side walls of the structure were monitored in the numerical analyses.

METHODOLOGY

Numerical analyses were performed using the two dimensional explicit FLAC v6.0 (Itasca, 2008) finite difference code. Ertugrul (2016) performed numerical analyses to investigate the racking behavior of box shaped embedded culverts with a numerical model validated against the results of previous dynamic centrifuge tests presented by Ozkan et al. (2013) and Ulgen et al. (2015). As part of the scope of the study performed by Ertugrul (2016), dynamic structural deformations and shear strains monitored during centrifuge tests were used to calibrate and validate the finite difference model. The centrifuge test set-up and the locations of the acceleration transducers in the backfill were shown in Fig. 1. Culvert models having different initial flexibility ratio (IFR) were tested in the centrifuge facility. Mechanical properties of the backfill material and structural attributes of the tunnel models used in the numerical modeling were taken in accordance with the
values reported by Ozkan et al. (2013). In Figure 2, racking ratio for tunnels with different initial flexibility ratio (IFR) were compared with those obtained from centrifuge tests. A good agreement was observed between centrifuge test data and results of numerical analyses. In the same figure, racking ratio values calculated with the analytical approach suggested by Penzien (2000) were presented for comparison purpose.

In the current study, the same validated numerical model was adapted to investigate the effect of a possible lateral soil arching due to installation of deformable geofoam cushions along the sidewalls of the shallow buried box section tunnels. Different from the previous work reported in the literature, in the current study, stiffness degradation and damping ratio of the soil were adopted as a function of soil strains and confining stress to represent the actual behavior in a more realistic way. In the finite difference analyses, plane strain box section models having dimensions of 2m×2m (width × height) embedded in sand were analyzed (Fig. 3). The soil was modeled as a homogeneous isotropic elasto-plastic material characterized by Mohr-Coulomb yield function with non-associated plastic flow rule. For the backfill material, friction angle is taken as 40°. Dilatancy angle (ψ) were assigned as 15° as suggested by Vermeer and de Borst (1984). For all of the geomaterial sets, a nominal cohesion value of 0.01 kPa was adopted to increase the stability of the numerical solution.

Box tunnel was represented by elastic beam-column elements whereas the soil medium was modeled with quadrilateral elements. Finite difference grid and initial boundary conditions for the investigated problem are shown in Figure 4. Static analysis was performed using an incremental loading procedure to facilitate proper simulation of geostatic stress conditions in the soil, installation process of the tunnel and stress redistribution after installation of the tunnel. In the numerical analyses were EPS geofoam panels of low stiffness were present, another stage of analysis were defined following the stage where placement of tunnel sections were simulated. Cross section sidewall and top-bottom slab thicknesses for the shaltunnel model are presented in Table 1.

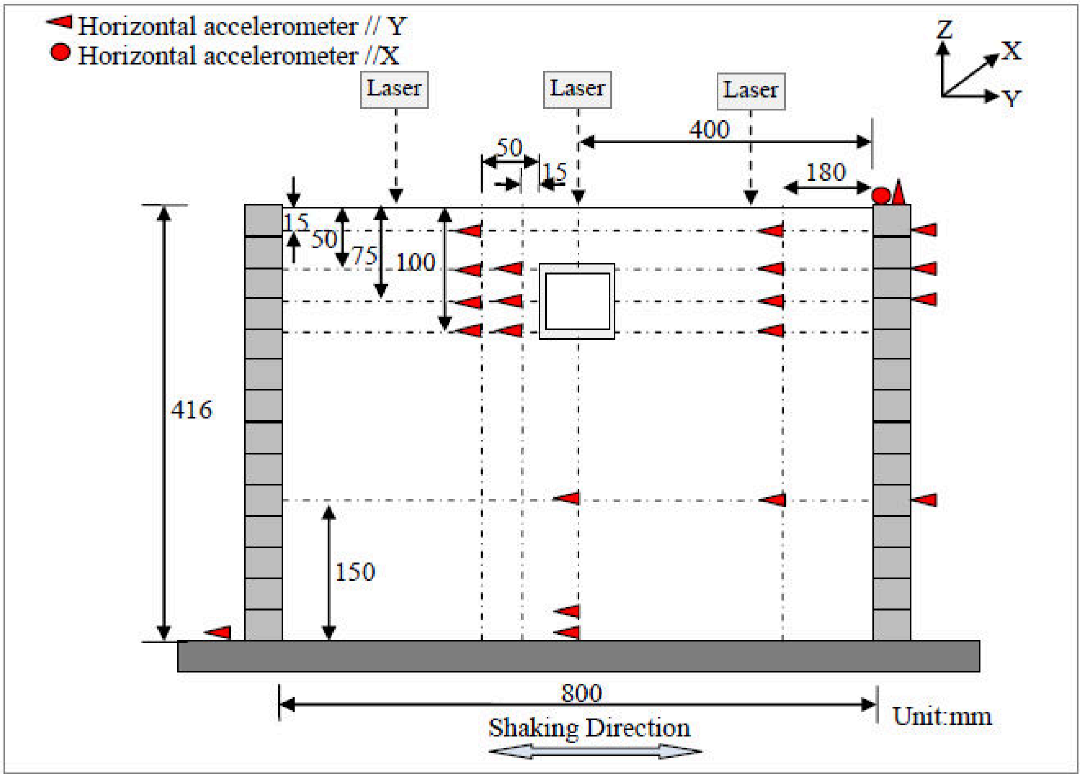

Figure 1. Centrifuge test set-up (Ozkan et al. 2013).

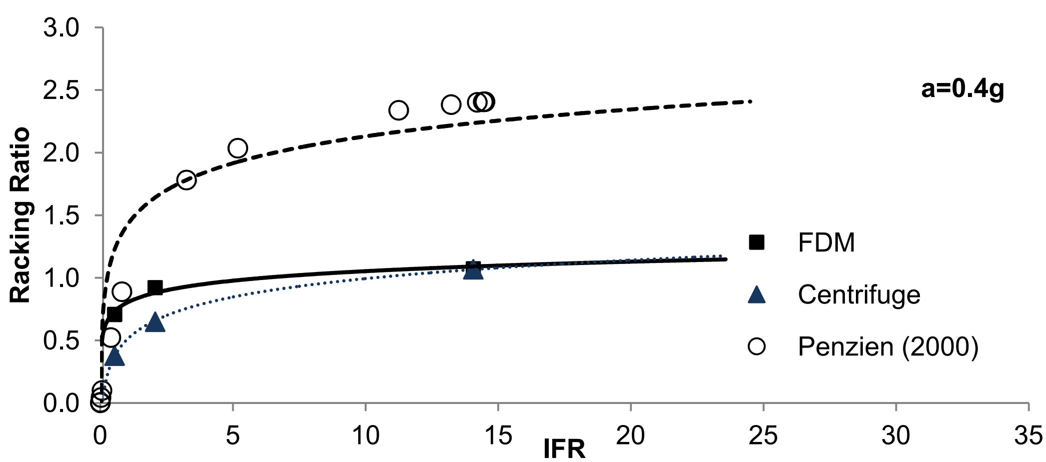

Figure 2. Variation of racking ratio with respect to flexibility ratio (Ertugrul 2016).

Parameter *IFR* in Table 1 is defined as the relative stiffness of the underground structure with respect to the non-deformed soil and is given by (Wang 1993):

$$IFR = \frac{G_{max}W}{SH} \tag{1}$$

where G_{max} is the maximum shear modulus of the soil, *W* and *H* are the width and height of the box tunnel and *S* is the force required for unit racking deformation of the structure itself. For single barrel tubes, this equation can be expressed as:

$$IFR = \frac{G_{max}}{24}\left(\frac{H^2W}{EI_W} + \frac{HW^2}{EI_R}\right) \tag{2}$$

where I_W and I_R are the moments of inertia of the sidewalls and top-bottom slabs, respectively. Elastic modulus of the C30 type concrete for an average compressive strength of 27.6 MPa is determined as 25.9 GPa based on the following equation:

$$E_c = 57000\sqrt{f_c} \tag{3}$$

where f_c is the compressive strength of concrete in psi. This elastic modulus value along with a unit weight of the tunnel of 23.6 kN/m^3 are typical properties for C30 concrete according to European Norms. Mechanical attributes of the structural elements are presented in Table 1. Stiffness characteristics of the analyzed structural model are representative for medium size box culverts or small tunnels considering the typical dimensions of embedded structures in field applications.

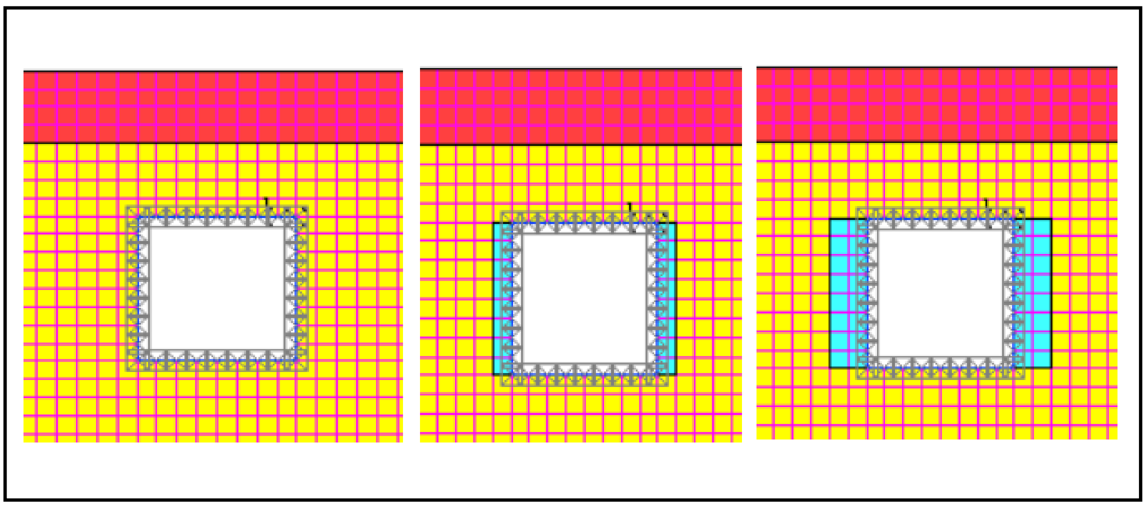

Figure 3. Numerical model of the embedded box section tunnel.

Numerical analyses were performed for tunnel models embedded at 2m and 6m depths (measured from the ground surface to the top slab) since embedment depth significantly affects the seismic response of the structure. Debiasi et al. (2013) indicated that effect of wall friction gains importance after a critical depth D_{co}, measured from ground surface to the top slab of the embedded structure. D_{co} is found to vary between 0.8L and 1.0L where L is the length of the side wall for box tunnels having aspect ratio of 1. The racking ratio of the box tunnels decreases as the interface between soil and structure becomes more rigid. This effect becomes more pronounced as the burial depth of the structure decreases. Hence, elasto-plastic Mohr-Coulomb interface elements were introduced at the wall-soil contacts within the analyses. Tiwari et al. (2010) conducted physical laboratory tests to investigate strength reduction at the interface between various soils and construction materials such as concrete, steel and wood. δ/ϕ ratio for sand-concrete interfaces is suggested as 0.94 where δ is the interface friction angle and ϕ is the internal angle of friction for the granular material. In the numerical analyses, δ values for the soil-structure interfaces are taken according to the δ/ϕ ratio (between sand and concrete) suggested by Tiwari et al. (2010). Geomaterial properties considered in the present numerical study are presented in Table 2.

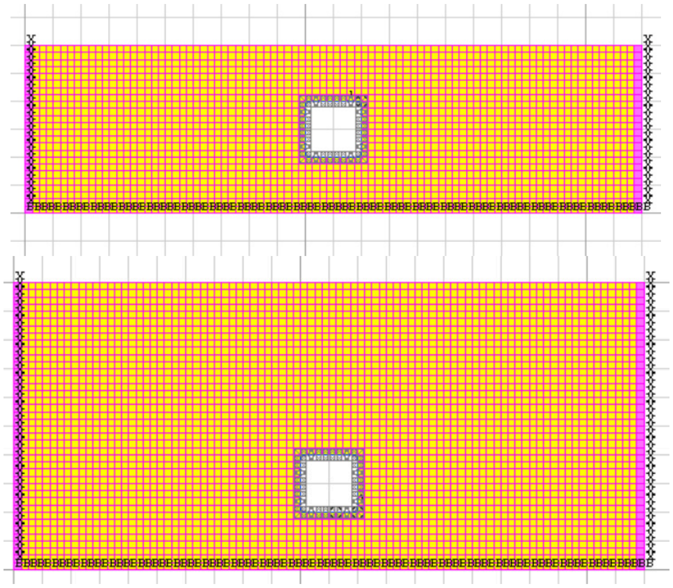

Figure 4. Finite difference grid (a) Embedment depth=2m (b) Embedment depth=6m.

Dynamic analyses were performed for two different base excitation cases. In the first case, a sinusoidal harmonic acceleration time history was applied to the lower most grid points of the model, to simulate earthquake-induced vertically propagating shear waves. The amplitude and frequency of this uniform base motion is taken as 0.1g and 3Hz. Silent boundary conditions were applied to the limits of the model to simulate wave propagation to outside of the model geometry. Although the application of earthquake excitations in physical modeling studies is considered more realistic, Bathurst and Hatami (1998) and Matsuo et al. (1998) reported that simple harmonic base excitations cause more aggressive impact on the structure compared to the effect of a real earthquake excitation with similar predominant frequency and amplitude. Additionally, application of harmonic base motion allows more accurate comparisons to be made regarding the effect of different input excitation parameters investigated in this study. In the second case of analysis, earthquake acceleration-time history recorded at Gebze Station during the devastating Kocaeli Earthquake (August 17, 1999) in Turkey was applied as input excitation.

Table 1. Geometry and structural attributes of the tunnel model.

Property	Sidewall	Top-Bottom slabs
Thickness (t_w) [mm]	100	320
Moment of Inertia (I) [m^4]	8.33×10^{-5}	2.73×10^{-3}
Elastic Modulus [kPa]	2.60×10^{7}	
Comp. Strength [kPa]	2.76×10^{4}	
Yield Strength [kPa]	4.13×10^{5}	
Lining Stiffness (k_l) [kPa]	1600	
IFR	8.95	
Embedment depth [m]	2m	

Table 2. Soil and geofoam properties.

Soil Shear Modulus [kPa]	5.65×10^4
Soil Bulk Modulus [kPa]	1.39×10^5
Soil Density [kg/m^3]	1600
Soil Friction Angle (°)	40
Soil Dilation Angle (°)	15
Soil Poisson's Ratio	0.30
Geofoam Density [kg/m^3]	20
Geofoam Elastic Modulus [kPa]	6000
Geofoam Poisson's Ratio	0.11
Soil-Structure Interface Friction Angle	0.94ϕ
Soil-Geofoam Interface Friction Angle	0.65ϕ

Shear modulus degradation and damping ratio curves for the soil were formulized based on the empirical relationships proposed by Ishibashi and Zhang (1993). In the dynamic analyses, geofoam relative thickness values (ratio of geofoam cushion thickness (*t*) to tunnel height, *H*) are taken as 0.125 and 0.250 for both of the embedment depths.

DISCUSSION OF THE RESULTS

According to Wang (1993), racking ratio (RR) of a tunnel is defined as the ratio of the racking deformations of the underground structure to the free field deformation of the ground at the relevant depth as depicted in Figure 5(a). For the estimation of the free field shear strains in the soil, numerical models without tunnel structure were analyzed. Penzien (2000) suggested the following relationship to estimate the racking ratio of the structure:

$$RR = \frac{4(1-\nu_s)}{1+\alpha_s} \tag{4}$$

$$\alpha_s = (3-4\nu_s)\frac{k_l}{k_{si}} \tag{5}$$

where ν_s is the Poisson's ratio of the soil, k_{si} and k_l are soil and lining stiffness coefficients, respectively. According to Penzien (2000), k_{si} is defined as the ratio of soil shear modulus to the height of the soil medium. Lining stiffness (k_l) for the finite difference model indicated at Table 1 was calculated through plane strain static analysis of the lining subjected to shear loading. For the tunnel models embedded at 2m and 6m below the ground surface, RR is calculated as 1.90 and 1.57, respectively according to Penzien (2000) approach. Based on the finite difference analyses, RR values are estimated as 1.81 and 1.43. It was observed that racking ratio estimations are in agreement with those of the analytical approach.

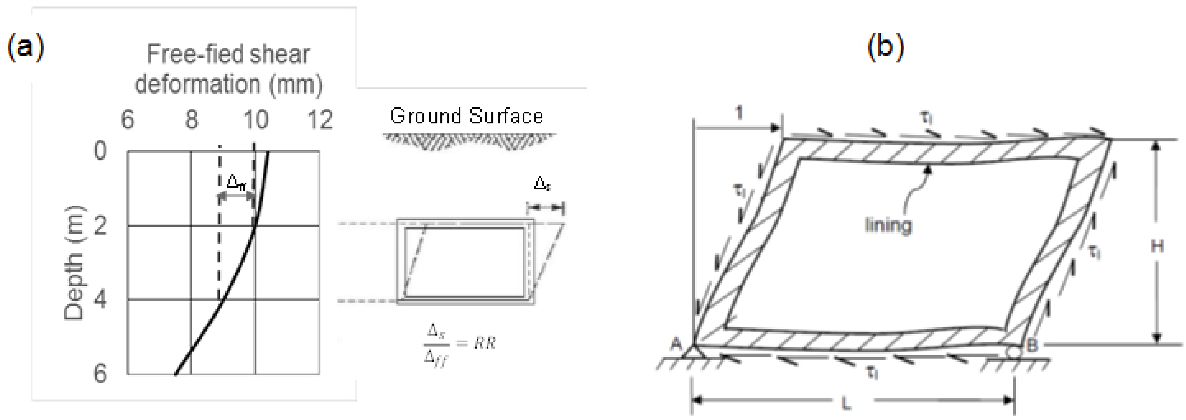

Figure 5. (a) Racking ratio of the box tunnel (Owen and Scholl, 1981) (b) Stiffness coefficient $k_l=\tau_l$ for a rectangular tunnel lining (Penzien 2000).

Dynamic thrust for the harmonic loading case is depicted in Figure 6. Geofoam side cushions provide reduction up to 25% in dynamic earth thrust for models with embedment depth of 2m, however the reduction effect diminished to only 4% for the tunnel embedded at 6m. For the real earthquake scenario (Fig. 7), the reduction in maximum seismic thrust reached up to 30% for tunnel at 2m below soil surface, and 24% for the model embedded at 6m. In Figure 8, time histories for the bending moments at the center of the sidewalls of the tunnel are shown. The maximum moments were reduced by approximately 22% and 33%, respectively for the tunnel models having embedment depths of 2m and 6m as a result of installation of geofoam cushions.

CONCLUSION

The present study discusses results of a series of numerical analyses addressing the dynamic behavior of box tunnels embedded in cohesionless soils. Effects of EPS geofoam cushions on the dynamic earth force and sectional forces in the structure were investigated by analyzing two dimensional finite difference models of a full-scale embedded box structure.

Time dependent racking deformations of the tunnels as well as bending moments and dynamic lateral earth pressures on the sidewalls of the structure were monitored in the numerical analyses. Installation of EPS geofoam cushions led to various amounts of earth force and displacement reductions compared to the results of the analyses without geofoam.

Relative structural rigidity of the embedded structure, embedment depth and the thickness ratio of the geofoam cushion played important roles in the reduction of the seismic lateral earth loads and racking deformations. Maximum seismic force was reduced by 30% for tunnel model with embedment depth of 2m. The reduction amount for the same structure embedded at 6m depth was 24%. A similar trend is observed for the bending moments along the walls of the structure during seismic event. The maximum moment was reduced by 33% for geofoam thickness ratio of 0.25. Embedment depth has a significant effect on the reduction amount of seismic forces by geofoam cushions. Numerical analyses indicate that the lateral dynamic arching effect that may be induced in the granular media as a result of lateral elastic deformations of the geofoam inclusion can provide reductions in the sectional forces in the structure which may lead to a more economical seismic design of box tunnels.

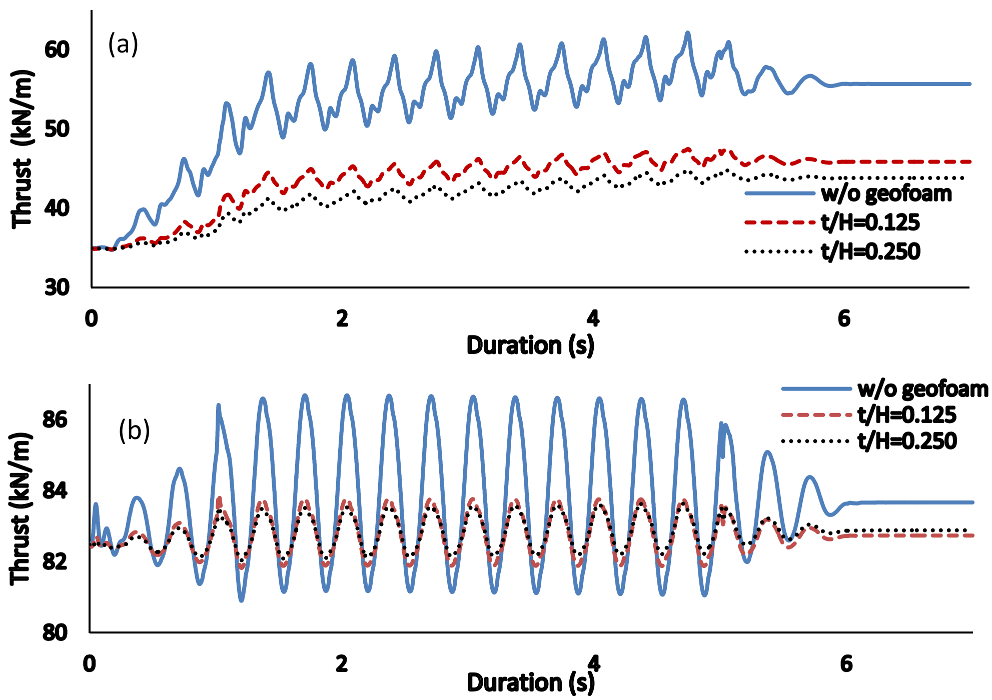

Figure 6. Time histories of dynamic earth force on the tunnel walls for harmonic loading case (a) Embedded at 2m depth (b) Embedded at 6m depth.

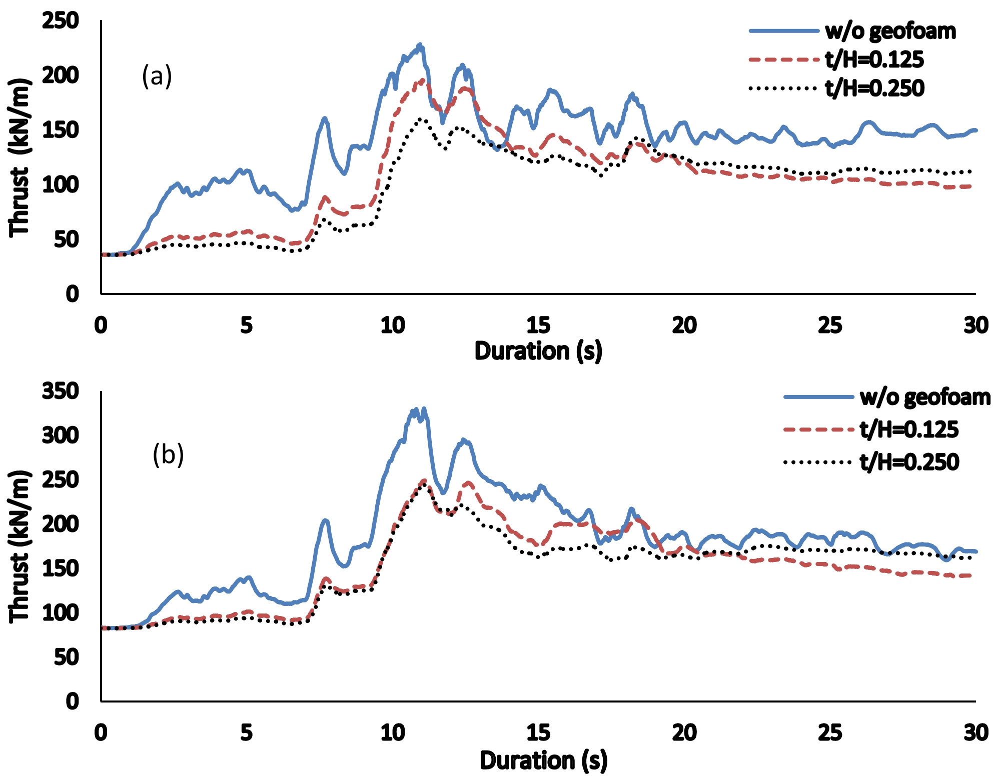

Figure 7. Time histories of seismic thrust on the tunnel walls for a real earthquake scenario (a) Embedded at 2m depth (b) Embedded at 6m depth.

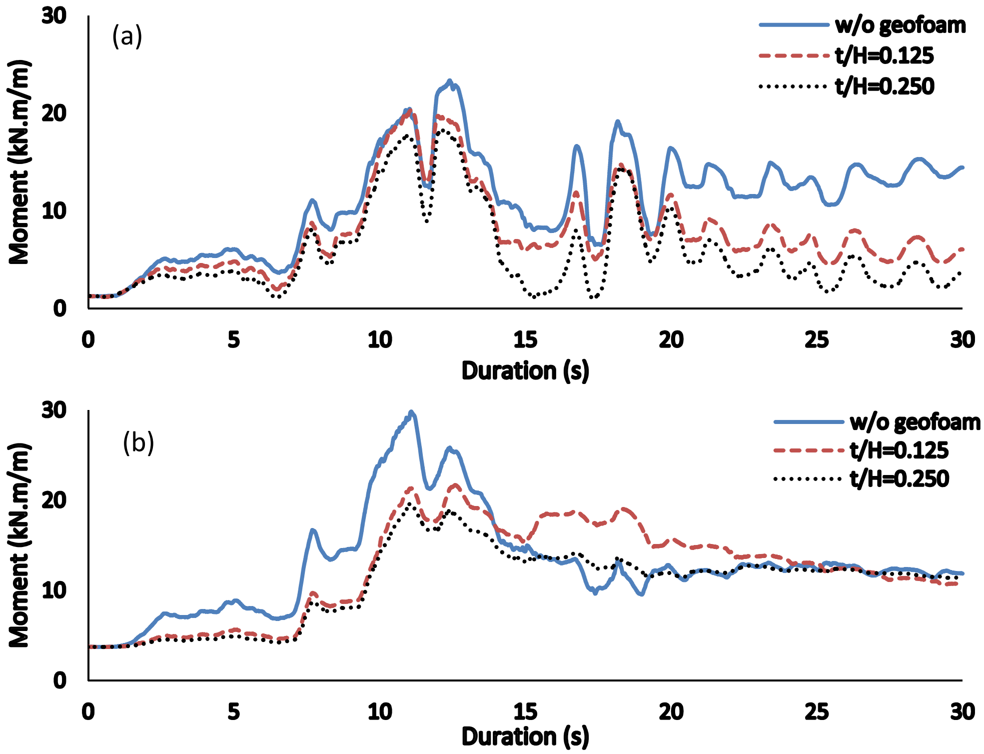

Figure 8. Time histories of seismic moment on the tunnel walls for a real earthquake scenario (a) Embedded at 2m depth (b) Embedded at 6m depth.

REFERENCES

Bobet A., Fernández, G. and Huo, H., (2008). "A practical iterative procedure to estimate seismic induced deformations of shallow rectangular structures." *Canadian Geotechnical Journal*, Vol. 45, No.7, pp. 923-938.

Debiasi, E., Gajo, A. and Zonta, D. (2013). "On the seismic response of shallow-buried rectangular structures", *Tunnelling and Underground Space Technology*, 38: 99-113.

Ertugrul, O. L., Trandafir, A. C. (2011). "Reduction of Lateral Earth Forces Acting on Rigid Non-Yielding Retaining Walls by EPS Geofoam Inclusions". *ASCE Journal of Materials in Civil Engineering*, 23(12), pp. 1711-1718.

Ertugrul, O. L., Trandafir, A. C. (2012). A Physical Modeling Study on the Dynamic Response of Flexible Retaining Walls with Deformable EPS inclusion. Proceedings of the 15th World Conference on Earthquake Engineering, Paper No.3474, Lisbon, Portugal, September 2012.

Ertugrul, O. (2016). "Numerical Modeling of the Seismic Racking Behavior of Box Culverts in Dry Cohesionless Soils", *KSCE Journal of Civil Engineering*, 20(5), pp. 1737-1746.

Huo, H., Bobet. A. and Fernandez, G. (2006). "Analytical solution for deep rectangular underground structures subjected to far field shear stresses." *Tunnelling and Underground Space Technology*, Vol.21, No.6, pp. 613–625.

Itasca Consulting Group, Inc., (2008). FLAC 2D Fast Lagrangian Analysis of the Continua Version 6.0 Dynamic Analysis User Manual, Minneapolis, Minnesota.

Ozkan, M.Y., Ulgen, D., Saglam, S., Vrettos C. and Chazelas J.L. (2013). Centrifuge Modeling of Dynamic Behavior of Box Shaped Underground Structures in Sand: Final Report. Seismic Engineering Research Infrastructures for European Synergies (SERIES), Project No: 227887.

Owen, G. N., and Scholl, R. E. (1981). Earthquake Engineering of Large Underground Structures, Federal Highway Administration, Report No: FHWA/RD-80/195.

Penzien, J. (2000). "Seismically induced racking of tunnel linings." *Journal of Earthquake engineering and structural dynamics*, Vol. 29, No.5, pp. 683–691.

Trandafir, A.C., Ertugrul, O. L. (2011). Earthquake Response of a Gravity Retaining Wall with Geofoam Inclusion. Proceedings of the Geo-Frontiers 2011, Geotechnical Special Publication No. 211, pp. 3177-3185, Dallas, Texas.

Ulgen, D. (2011). An experimental study on the behavior of box-shaped culverts buried in sand under dynamic excitations, Ph.D. Dissertation, Middle East Technical University, Ankara, Turkey.

Ulgen, D., Saglam, S., Ozkan, M.Y. (2015). "Dynamic response of a flexible rectangular underground structure in sand: centrifuge modeling", *Bulletin of Earthquake Engineering*, 13(9), pp.2547-2566.

Vermeer, P.A., De Borst, R. (1984). "Non-associated Plasticity for Soils, Concrete and Rock" Heron, 29(3), 64 pp.

Wang, J.N. (1993). Seismic design of tunnels, Parsons Brinckerhoff, Inc., Monograph 7.

Selection of Soil Stiffnesses for the Load Rating of In-Service Culverts

S. Mehdi Mousavi[1]; Priyantha W. Jayawickrama, Ph.D., M.ASCE[2]; Timothy A. Wood Ph.D.[3]; and William D. Lawson, P.E., Ph.D., M.ASCE[4]

[1]Graduate Research Assistant, Dept. of Civil, Environmental, and Construction Engineering, Texas Tech Univ., Lubbock, TX 79409. E-mail: m.mousavi-ghorabaee@ttu.edu
[2]Associate Professor, Dept. of Civil, Environmental, and Construction Engineering, Texas Tech Univ., Lubbock, TX 79409. E-mail: priyantha.jayawickrama@ttu.edu
[3]Assistant Professor, Dept. of Civil and Environmental Engineering, The Citadel, Charleston, SC 29409. E-mail: twood3@citadel.edu
[4]Associate Professor, Dept. of Civil, Environmental, and Construction Engineering, Texas Tech Univ., Lubbock, TX 79409. E-mail: william.d.lawson@ttu.edu

Abstract

This paper presents findings from a critical review and an analytical study of soil stiffness values for the load rating of reinforced concrete box culverts. The responses of the soil-culvert system under dead and live loads were examined separately for a production-simplified, two-dimensional, linear elastic, soil-structure interaction model. First, soil-culvert systems were analyzed to determine dead-load-induced moments in the structure. The results were compared with moments obtained from an AASHTO policy-based structural-frame model and a calibrated value of static soil modulus, E = 10 ksi was selected as the optimum. A comprehensive literature review evaluated reasonable soil stiffnesses for live load analysis in culvert load rating. Typical resilient moduli of 12, 24 and 36 ksi for low, medium and high-quality culvert backfill soils were identified for live load predictions in the soil-structure interaction model.

INTRODUCTION

Load rating is the analytical process of identifying the largest vehicle load that can safely cross a bridge, or, for this paper, a bridge-class culvert. Load rating culverts requires that the structure be analyzed to determine moments, shear forces and axial loads induced by both dead loads and live (traffic) loads. Culvert load rating depends on the interaction between culvert capacity, dead load, and live load as seen in the rating factor equation for the Load Factor Rating method (AASHTO 2015a).

$$RF = \frac{C - A_1 D}{A_2 L(1+I)} \quad (1)$$

where:

A_1 = Factor for dead loads
A_2 = Factor for live load
C = Capacity
D = Dead load effect
I = Impact factor
L = Live load effect

The dead and live load demands on the structure are determined by analytical modeling. Modeling can be approached in many ways, with each analytical method requiring its own